„From molecules to functional architecture. Supramolecular interactions"
Edited by V.I. Rybachenko
Donetsk 2012, East Publisher House, ISBN 978-966-317-155-5

Chapter 3

The influence of aggregates of calixarenes and dendrimers on the protolytic equilibria of dyes in aqueous solution

N.A. Vodolazkaya[a], N.O. Mchedlov-Petrossyan[a], L.N. Bogdanova[b], R.V. Rodik[c] and V.I. Kalchenko[c]

[a] *Department of Physical Chemistry, V. N. Karazin Kharkov National University, Svoboda sq. 4, 61022, Kharkov, Ukraine*

[b] *Pharmstandart-Biolik, Pomerki 70, 61084, Kharkov, Ukraine*

[c] *Institute of Organic Chemistry, National Academy of Science of Ukraine, Kiev, 02094, Ukraine*

1. Introduction

Nowadays, the synthesis and application of water-soluble receptor molecules, such as crown ethers, cryptands, calixarenes, dendrimers, etc., belong to the most important tasks of supramolecular chemistry [1]. The solubility in water is usually achieved by attaching ionic groups to the molecules [2–6]. Further interactions of thus modified receptors, in particular calixarenes, with various substrates (either molecules or ions) in aqueous media are usually considered only in terms of "host + quest" association [7–13].

Meanwhile, large cavity-bearing molecules, among them those containing charged groups, are able to form own aggregates (or associates, micelles, clusters) in water [4, 5, 14–24] because of hydrophobic interactions. Therefore apart from "host + quest" supramolecular interactions, micellar effects should be taken into account. The last effects and their influence on the state of compounds dissolved in water are considered in full for the case of well-established micellar solutions of colloidal surfactants [25]. The non-aqueous microenvironment in concert with the interfacial micellar charge display a specific kind of modification of the properties of substrates bound to the micellar pseudophase [25]. However, the corresponding information concerning the supramolecular systems is lacking.

In order to fill a gap in our knowledge of this issue, we conducted a series of systematic studies with cationic calixarenes and dendrimers in aqueous media [26–31]. The brief review given in this chapter is aimed to summarize the main results.

In Figures 1 and 2, the calixarenes and dendrimers examined in our studies are presented. As suitable tools for such a study we used a set of organic dyes: acid-base and solvatochromic indicators and luminophores.

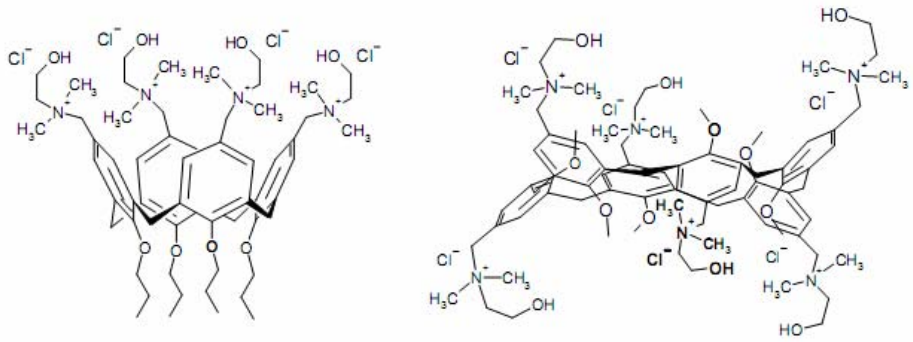

1 **2**

*Figure 1. 5,11,17,23-tetrakis(N,N-dimethyl-N-hydroxyethylammonium)-methylene-25,26,27, 28-tetrapropoxy-calix[4]arene tetrachloride (**1**) and 5,11,17,23,29,35-hexakis(N,N-dimethyl-N-hydroxyethylammoniummethylene)-37,38,39,40,41,42-hexametoxycalix[6]arene hexachloride (**2**) in their most probable conformations.*

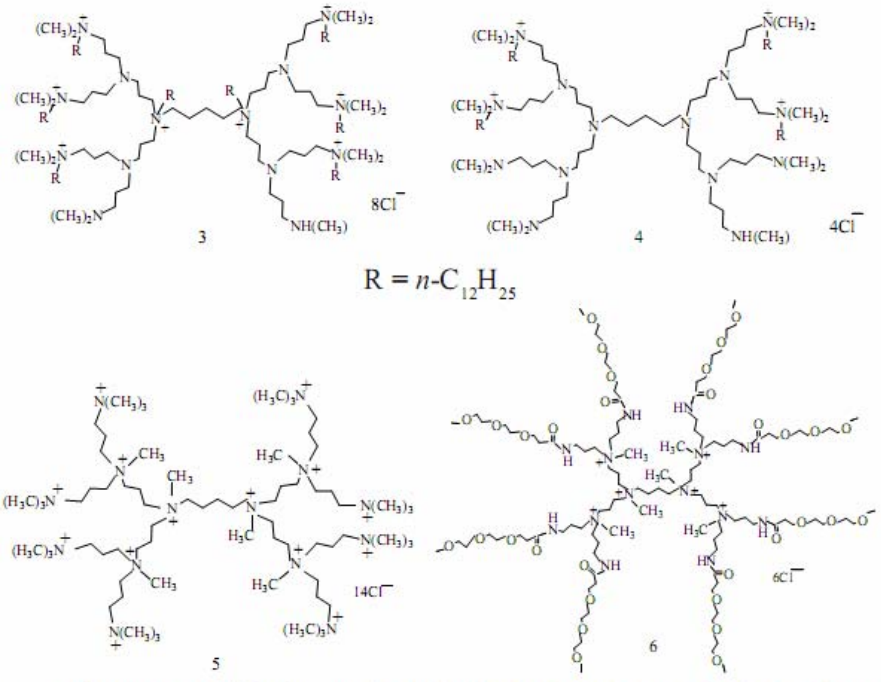

3 4

$R = n\text{-}C_{12}H_{25}$

5 6

*Figure 2. The structure of dendrimers (**3** – $D(8)(CH_3)_{16}(C_{12}H_{25})_8$, **4** – $D(8)(CH_3)_{16}(C_{12}H_{25})_4$), **5** – PMD(8), **6** – IMD8-CO-MPEG).*

2. Phenomenological approach: the shift of the acid-base equilibria caused by ionic dendrimers and calixarenes

Indicator dyes are common molecular probes for studying surfactant micelles, droplets of microemulsions, phospholipid liposomes, etc. because of high sensitivity of their spectral and acid-base properties to the nature of the microenvironment [25]. Such dyes were also often used in the research of the properties of receptor molecules [7, 9, 11, 12]. However, in the cited papers the interactions of the receptor cavity with the dye molecule (or ion), i.e., the "host + quest" interactions, have primarily been taken in consideration.

In order to investigate the aqueous solutions of the above calixarens and dendrimers as media for the acid-base reactions, we utilized over twenty organic dyes [26–31].

For example, the relatively small-sized prolonged indicator molecules are represented by methyl orange (Figure 3). In principle, such species may be docked into the calixarene cavity.

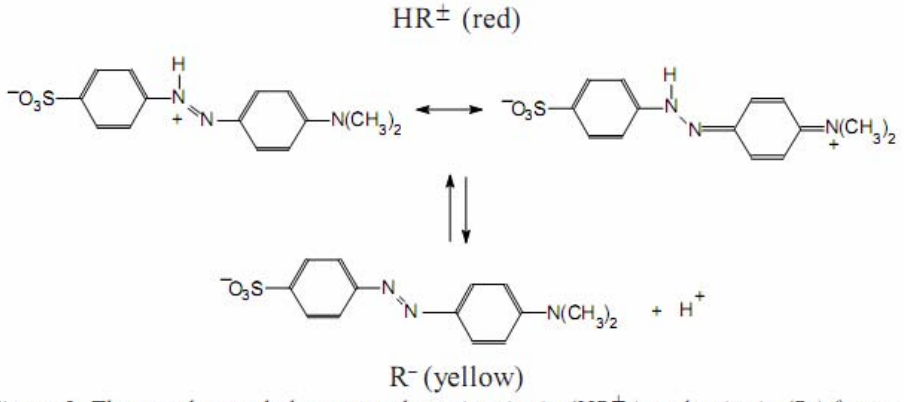

Figure 3. The azo dye methyl orange: the zwitterionic ($HR^{\pm}$) and anionic (R^{-}) forms.

The standard acid-base sulfonephthalein indicators phenol red ($X^1 + X^2 = X^3 = H$) and especially its derivatives, such as bromophenol blue, thymol blue, and bromothymol blue (Figure 4), are certainly too large to be involved to high extent into the host cavity, at least in the case of the calixarenes under study [26, 31]. Besides these indicators, methyl yellow, neutral red, four nitrophenols, as well as fluorescein (Figure 5) and its derivatives eosin, rose Bengal B, decylfluorescein, and some other dyes were also involved in the investigation.

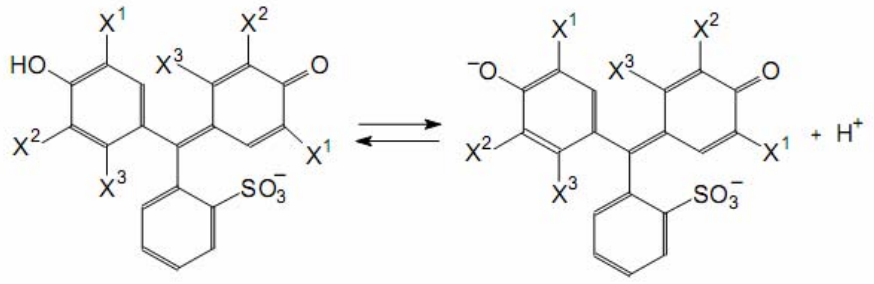

HR⁻ (yellow) R^{2-} (red or blue)

Figure 4. The monoanionic (HR^-) and dianionic (R^{2-}) forms, sulfonephthalein dyes.

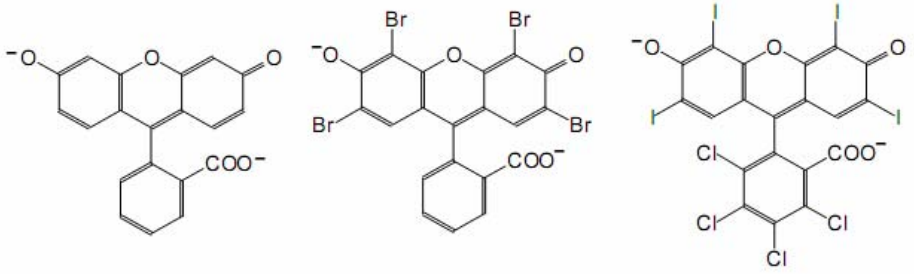

Figure 5. The R^{2-} forms of fluorescein, 2,4,5,7-tetrabromofluorescein (eosin), and 2,4,5,7-tetraiodo-3',4',5',6'-tetrachlorofluorescein (rose Bengal B).

As a key quantitative characteristic, the so-called "apparent" pK_a^{app} value of the indicator dye was determined by means of visible spectroscopy accompanied by potentiometric pH determination [25]. Normally, the concentration of indicator dyes in solutions is chosen in the region of 1×10^{-5} M. The concentration of the dendrimer or calixarene was as a rule within the range of 1×10^{-5} to 0.01 M.

In brief, our investigations [26–31] have demonstrated that appearance of cavity-bearing species **1-6** in solution causes the same effects as the introduction of cetyltrimethylammonium bromide (CTAB), *N*-cetylpyridinium chloride (CPC), etc. The pK_a^{app} shifts against the pK_a in water (pK_a^w) are of the same direction and close by value to those registered in micellar solutions of cationic surfactants.

The pK_a^{app} values of indicators in solutions of dendrimers [27] are exemplified in Table 1, and some data for calixarene solutions [28] are

compiled in Table 2. The symbols pK_a^w and pK_a^{w*} denote the indices of the thermodynamic dissociation constants in water and of the constants at the given ionic strength, *I*, respectively.

Table 1. The pK_a^{app} values of different indicator dyes in 1.2×10^{-4} M solutions of dendrimer **3** *($I \approx 0.01$ M) and cationic surfactants, CPC and CTAB [27]*

Dye (pK_a^w)	pK_a^{app}	ΔpK_a^{app}	ΔpK_a^{app} in surfactant micelles
Bromophenol blue (4.20)	2.19 ± 0.04	–2.01	–(1.94–2.16)
Decylfluorescein (6.31)	4.92 ± 0.03	–1.39	–(1.37–1.39)
Bromothymol blue (7.30)	6.42 ± 0.04	–0.88	–(0.71–0.94)
Thymol blue (9.20)	8.50 ± 0.03	–0.70	–(0.30–0.37)

The medium effects (here: the $\Delta pK_a^{app} = pK_a^{app} - pK_a^w$ values) are governed rather by the charge type of the acid-base couple and the nature of the ionizing group, than by the size of the dye ions and molecules. This strongly resembles the well-documented interaction of dyes with micelles of cationic surfactants [25]. The dependence of the pK_a^{app} values on the concentration of the receptor molecules and the alteration of the absorption spectra of the equilibrium forms of the indicators as compared with those in water are typified in Figures 6 and 7 respectively.

Such type of dependences and absorption band shifts are also registered for sulfonephthalein indicators in the presence of cationic surfactants.

Hence, the medium effects for a number of indicator dyes in solutions of **1-6**, on the one hand, and in micellar solutions of common cationic surfactants, on the other hand are similar. This allowed deducing that the dyes may interact with the species **1-6** as with cationic micelles. Even more possible seemed to be the formation of positively charged aggregates and the dye + aggregate interactions.

Table 2. The indices of the apparent ionization constants of acid–base indicators in 2.510^{-3} M aqueous solution of calixarene **1***; I = 0.05 M (NaCl + buffer) [28]*

Indicator	Charge type	pK_a^{w*} (pK_a^{w})	pK_a^{app} in **1** solution	ΔpK_a^{app}
Neutral red	A^+B^0	6.47 ± 0.04 (6.50)	6.41 ± 0.05	≈ 0
Thymol blue	AB^-	1.49 ± 0.01 (1.70)	0.29 ± 0.13 [a]	–1.41
Methyl orange	AB^-	3.21 ± 0.02 (3.40)	1.88 ± 0.05 [b]	–1.52 [–2.18] [b]
Methyl yellow	A^+B^0	3.06 ± 0.05 (3.25)	2.57 ± 0.04	–0.68
2,4-Dinitrophenol	A^0B^-	3.81 ± 0.02 (4.11)	2.88 ± 0.05	–1.23 [–1.46] [c]
2,6-Dinitrophenol	A^0B^-	3.58 ± 0.01 (3.71)	3.24 ± 0.01	–0.47
2,5-Dinitrophenol	A^0B^-	5.08 ± 0.02 (5.15)	4.52 ± 0.05	–0.63
4-Nitrophenol	A^0B^-	7.07 ± 0.04 (7.15)	7.08 ± 0.12 [d]	–0.07 [–0.81] [d]
Bromophenol blue	A^-B^{2-}	4.05 ± 0.02 (4.20)	2.59 ± 0.06 [e]	–1.61 [–1.59] [e]
Bromocresol green	A^-B^{2-}	4.85 ± 0.01 (4.90)	4.14 ± 0.05	–0.76
Bromocresol purple	A^-B^{2-}	6.30 ± 0.02 (6.40)	5.51 ± 0.10	–0.89
Bromothymol blue	A^-B^{2-}	7.26 ± 0.02 (7.30)	6.82 ± 0.03	–0.48
Phenol red	A^-B^{2-}	7.97 ± 0.02 (8.00)	7.40 ± 0.06 [f]	–0.60 [–0.93] [f]
ortho-Cresol red	A^-B^{2-}	8.25 ± 0.01 (8.46)	7.58 ± 0.04	–0.88
meta-Cresol purple	A^-B^{2-}	8.55 ± 0.01 (8.70)	8.28 ± 0.05	–0.42
Thymol blue	A^-B^{2-}	9.07 ± 0.02 (9.20)	9.14 ± 0.02	–0.06

[a] I > 0.05 M; [b] at **1** *conc. 0.01 M, pK_a^{app} of methyl orange equals 1.22 ± 0.05; [c] at* **1** *conc. 7.5 × 10^{-3} M, pK_a^{app} of 2,4-dinitrophenol equals 2.65 ± 0.04; [d] at* **1** *conc. 0.01 M, pK_a^{app} of 4-nitrophenol equals 6.34 ± 0.17; [e] at* **1** *conc. 0.01 M, pK_a^{app} of bromophenol blue equals 2.61 ± 0.05; [f] at* **1** *conc. 0.01 M, pK_a^{app} of phenol red equals 7.07 ± 0.01.*

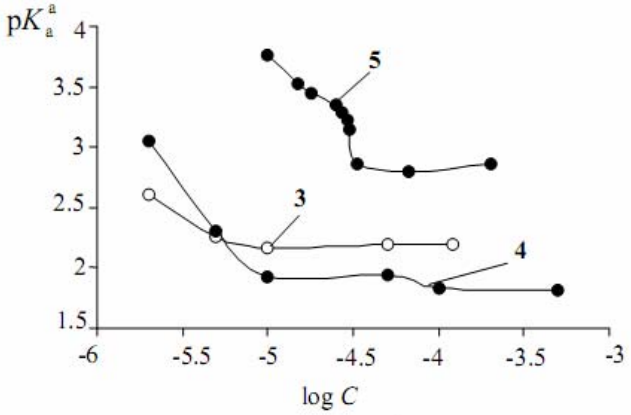

Figure 6. The dependence of bromophenol blue pK_a^a *values in solutions of* ***3***, ***4***, *and* ***5*** *on logarithm of dendrimer concentration. Dye concentration: 8.5×10⁻⁶, 9.0×10⁻⁶, and 5.0×10⁻⁶ M respectively;* C_{HCl} *varies from 0.001 to 0.01 M. Reprinted from ref. 27 with permission of the American Chemical Society.*

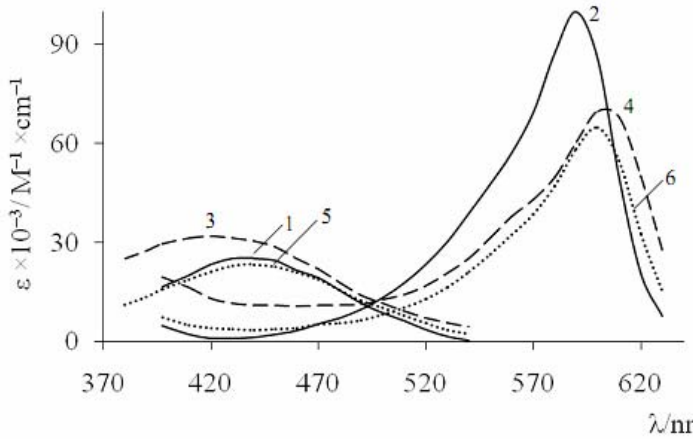

Figure 7. The absorption spectra of bromophenol blue anions HR^- *(1, 3, and 5) and* R^{2-} *(2, 4, and 6) in water (1, 2) and in the presence of (2.5–5.0)×10⁻³ M of calixarenes 1 (3, 4) and 2 (5, 6); pH = 8 (2) and 6 (4, 6), I = 0.05 M (buffer + NaCl). The spectra (1, 3, and 5) are obtained in the presence of 0.1–0.3 M HCl. Reprinted from ref. 31 with permission of the American Chemical Society.*

3. The evidences of the presence of aggregates in aqueous solutions of calixarene and dendrimers

The method of dynamic light scattering (DLS) allows revealing the existence of small aggregates with diameter around 3–4 nm in solutions of compound **1** [28, 29, 31]. For this calixarene, the aggregates are formed only if the concentration exceeds some threshold value. Such behavior strongly resembles the micelle formation of colloidal surfactants, and the abovementioned concentration is in fact the threshold, or critical aggregate concentration (CAC), analogous to the critical micelle concentration (CMC) of amphiphilic surfactants.

The similarity becomes even more expressed by comparing these CAC in solutions with and without addition of indifferent salts. In Figure 8, the intersection of the two straight lines in the intensity data corresponds to the critical aggregate concentration.

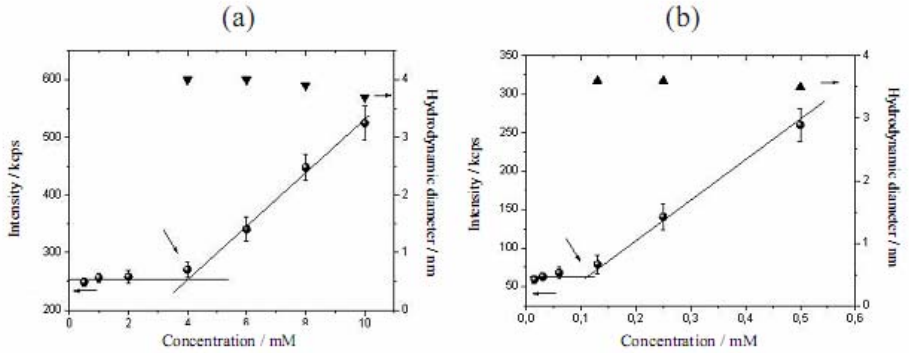

*Figure 8. The plots of the intensity of scattered light (in kilo counts per second) and hydrodynamic diameter obtained for the solutions of calixarene **1** prepared in deionized water (a) and in 0.05M NaCl aqueous solution (b) Reprinted from ref. 29.*

The threshold values thus obtained are 4×10^{-3} and 1.2×10^{-4} M in pure water and 0.05 M NaCl solution. Such a dramatic decrease in the CAC values emphasizes the similarity between compound 5 and colloidal surfactants. Indeed, the expressed decrease in the CMC values caused by indifferent salts is typical for common ionic amphiphiles, such as CTAB or CPC [25].

The measurements of the electrophoretic potential are also helpful. In the case of calixarene **1** in pure water, the ζ value varies within the range of + (60 to 80) mV [28, 29, 31]. The evident origin of the positive charge is the location of a fraction of Cl^- ions outside the colloidal aggregates. This also underlines the similarity between the calixarene aggregates and micelles of cationic surfactants.

In aqueous solutions of dendrimers **3** and **4**, aggregates of different sizes (5 to 3700 nm) have been detected under acidic and basic conditions, at concentrations similar to those used for the study of the indicator dyes (Table 3) [27]. The diameters of a major component of dendrimer **4** having four *n*-dodecyl chains correspond either to single molecules or to very small aggregates at both pH 10 and 2. On the other hand, dendrimer **3** bearing eight *n*-dodecyl chains is highly aggregated at pH 2 and 10 and show bimodal and trimodal size distributions. The data collected in Table 3 demonstrate that dendrimer **4** exists in water predominantly in the form of small-sized species even at concentrations above the CAC [27].

Table 3. Sizes of dendrimer aggregates in water at 25°C from dynamic light scattering

Dendrimer	C/M	pH	diameter/nm [a]
3	1.20×10^{-4}	2.0	293 (88%), 4900 (11%)
3	1.20×10^{-4}	10.0	64 (32%), 302 (32%), 3700 (35%)
4	5.09×10^{-4}	2.0	5 (major), 196 (minor)
4	5.09×10^{-4}	10.0	4.5 (major), 290 (minor)

[a] *Size distribution by volume percent. Size was not calibrated, and relative volumes were unreliable for the 5 nm diameter particles. Reprinted from ref. 27 with permission of the American Chemical Society.*

In the case of calixarenes, we also observed a significant dependence of aggregate properties on compound structure. The dramatic difference between the aqueous solutions of calixarenes **1** and **2** consists in the size of the aggregates. Indeed, the particles of the six-member calixarene are much larger. Their size varies within the range of $\approx 10^2$ to $\approx 10^3$ nm (Figure 9).

Such difference is probably caused first of all by the character of major conformations of the calixarenes (cone for compound **1** and 1,3,5-alternate for **2**). The less expressed hydrophobicity of the alkoxyaryl portion of calixarene **2** as compared that of compound **1** should be also taken into account.

The histogram for this polydisperse system is typified in Figure 9; for nine C_{calix} values from 1×10^{-4} to 0.01 M, the picture is similar in outline. Note, that the rather large particles of calixarene **2** as 1,3,5-alternate already exist in extremely diluted solutions (about 1×10^{-5} M) of this calixarene. Thus, it is difficult to reveal any distinct CAC value.

At the same time, the electrophoretic study of solutions of calixarene **2** in pure water demonstrated the existence of particles possessing positive charge, with the electrokinetic potential (zeta potential) value ζ = +(41–50) mV

lower as compared with that of calixarene **1** aggregates: +(60–80) mV. The ill-expressed decrease in ζ at higher C_{calix} values (insert in Figure 9) should be explained by the screening of the interfacial charge of the aggregates by the Cl^- ions, because the concentration of the latter in the bulk increases along with the increase in C_{calix}, a phenomenon well known for ionic surfactant micelles [25, 31] ("negative adsorption").

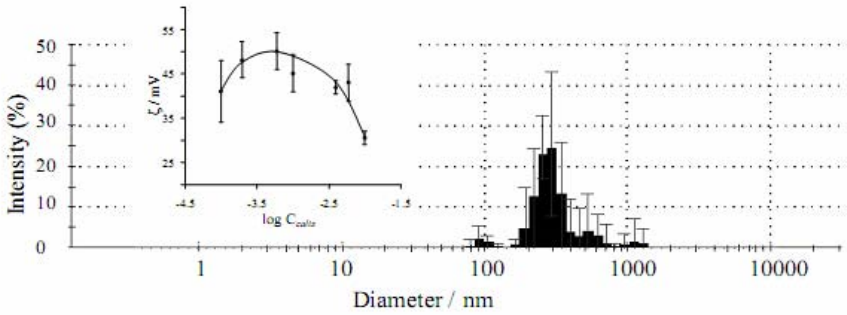

Figure 9. The DLS data: the size distribution by scattering intensity in aqueous solutions of calixarene **2**, $C_{calix} = 4\times10^{-3}$ *M, 25 °C. The insert demonstrates the variations of the electrokinetic potential along with the concentrations of calixarene* **2**. *Reprinted from ref. 31 with permission of the American Chemical Society.*

The transmission electron microscopy (TEM) data obtained within the wide concentration range of the colloidal systems confirm the polydisperse character and (in outline) the size of the calixarene aggregates studied (Figure 10).

It is evident, that the particles formed by calixarene **2** consist of primary aggregates, which are rather isometric than prolonged ones, with diameter ca. 15–40 nm (Fig. 10*a,b*). The particulates are amorphous. The formation of some part of secondary aggregates as a result of water evaporation during the sample preparation for the TEM experiments also cannot be excluded. However, just the secondary aggregates shown in Figure 10*a* (several typical examples from a much larger body of data) get the size range estimated by the DLS method. From such a picture, it can be deduced that the aggregates are in fact clusters of neutral salt molecules, i.e., six-charged cations with six chloride anions. Only the interfacial Cl^- ions can leave the aggregates, thus causing their positive charge. This hypothesis was supported by the measurements with the Cl^--selective electrode [31].

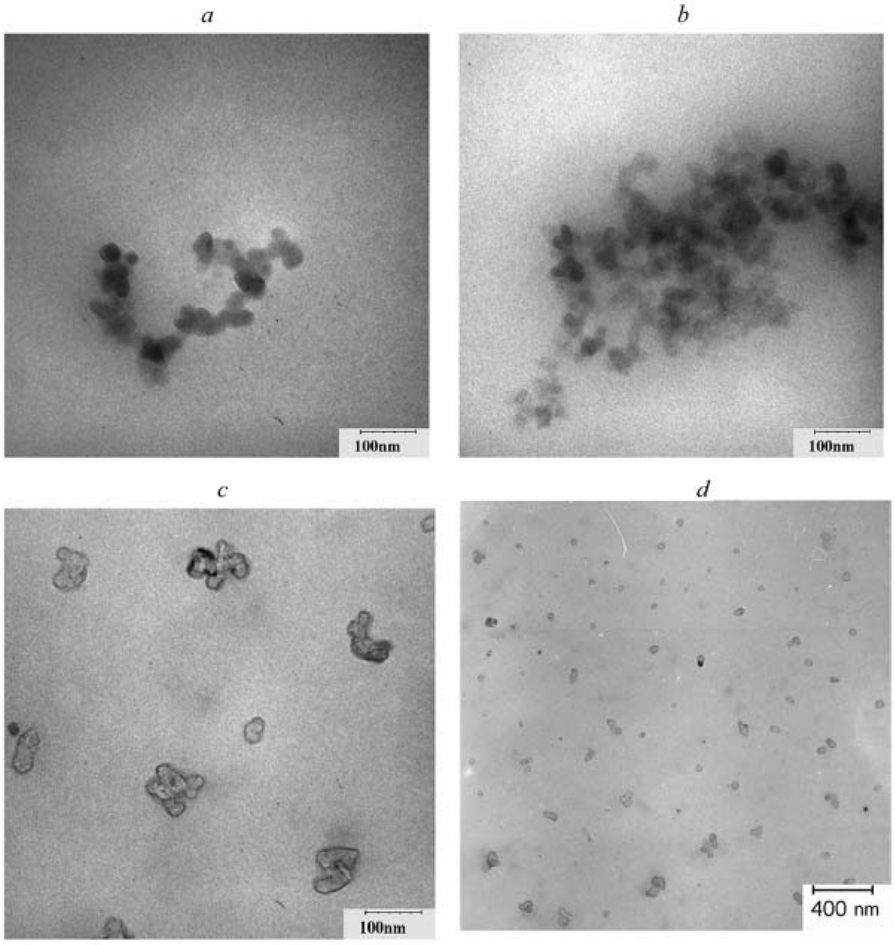

Figure 10. Typical electron micrographs of the aggregates of calixarenes **2** *(**a**, **b**) and* **1** *(**c**, **d**). The images **a** and **b** refer to the dried aqueous solutions (0.001 M); the images **c** and **d** were obtained using the 0.004 M solutions of calixarene* **1** *contrasted by rose Bengal B. Reprinted from ref. 31 with permission of the American Chemical Society.*

The differences in the behavior of calixarenes **1** and **2** probably originate from the peculiarity of their conformations. For calixarene **1** the cone, or, more precise, a dynamic equilibrium between two equivalent conformations of a pinched cone is typical. Its spatial structure investigated with molecular mechanic computations (MM+) [26] revealed that in vacuum two distal rings are almost parallel. Two other rings are almost orthogonal. Distances between distal N-atoms are equal to 0.59 and 1.37 nm, neighboring N-atoms are located

at 0.73 nm.

In contrast, the six-member calixarene **2** is conformationally mobile, and in its solutions the free rotation of the aromatic rings around the bonds with the $-CH_2-$ groups takes place, resulting in 1,3,5-alternates. For solutions of **2** in DMSO, it was proved by a sole spread signal at 3.98 ppm of methylene protons in ^1H NMR spectrum in DMSO [31]. In the crystal state, the 1,3,5-alternate conformation is also energetically more beneficial as compared with the cone or partial cone conformations [31].

Spatial structure of calixarene **2** in vacuum was studied by the molecular mechanic computations (MM+) method. Calixarene exists in a centrosymmetrical 1,3,5-alternate conformation. Three pairs of distal rings are allocated in almost antiparallel directions; corresponding dihedral angles are 28.6°, 17.95° and 3.93°. Two ammonium moieties are partly incorporated in the cavity of the macrocycle, distances between N-atoms are within 0.53 to 1.53 nm [31].

Recently [31], we compared our data with the results of other research groups devoted to the aggregates formed by cationic [6, 15, 17, 20, 32, 33] and anionic [4, 34] calixarenes.

4. The origin of the medium effects in aqueous solutions of cationic calixarenes and dendrimers

On the whole, the introduction of cationic calixarenes and dendrimers into the aqueous buffered solutions of the indicator dyes leads to their pK_a^{app} decrease. In addition to Tables 1 and 2, some data for most common indicator dyes are exemplified in Table 4.

Analogous effects at the transfer from water to calixarenes and dendrimers solutions were also recorded for other indicators. It confirms the colloid character of the systems under study and demonstrates the great significance of micellar effects in supramolecular systems.

The difference pK_a^{app} values and the values in water can be expressed through the transfer activity coefficients from water to pseudophase, or dispersed phase, ${}^w\gamma^m$, and electrical potential, Ψ [25]:

$$\Delta pK_a^{app} = pK_a^{app} - pK_a^{w} = \log \frac{{}^w\gamma_R{}^m}{{}^w\gamma_{HR}{}^m} - \frac{\Psi F}{2.302\,RT} \qquad (1)$$

The positive ς and, correspondingly, Ψ values of the colloidal systems explain the increase in the "apparent" acidic strength documented in Tables 1,

2, and 4. At that, the six-member calixarene displays a less expressed influence on the protolytic equilibria. This is in line with the fact that the ζ values for aggregates of compound **2** are ≈(20–30) mV lower as compared with those of **1**.

Table 4. The pK_a^{app} *values [±(0.01 to 0.07)] of different indicator dyes in aqueous solutions of calixarenes and dendrimer* **3**, *25 °C*

System [a]	pK_a^{app} [$\log(K_a^{app}/K_a^{w*})$]			
	Phenol red	Bromophenol blue	Bromothymol blue	Methyl orange
Water, I = 0.05 M	7.97	4.05	7.26	3.21
Calixarene **1**	7.40 [0.57]	2.59 [1.46]	6.82 [0.44]	1.88 [1.33]
Calixarene **2**	7.66 [0.31]	2.90 [1.15]	–	2.64 [0.57]
Dendrimer **3**	–	2.19 [1.86]	6.42 [0.84]	–
Micellar solution of cationic surfactants	7.08 [b] [0.89]	2.83 [c] [1.22]	6.36 [b] [0.90]	1.00 [c] [2.21]

[a] *Conc. of calixarenes: 2.5×10⁻³ M, I = 0.05 M; conc. of dendrimer* **3***: 1.2×10⁻⁴ M (the CAC value is 9.0×10⁻⁵ M), I = 0.01 M; the* pK_a^{app} *values are determined in buffer or HCl + NaCl solutions;* [b] *CPC: 0.003 M, I = 0.05 M (buffer + KCl).* [c] *CTAB: 0.003 M, I = 0.05 M (buffer or HCl + KBr).*

Note, that the ΔpK_a^{app} values are quite different for different charge types of acid-base couples, for the indicators of different structure, or even for sulfonephthaleins bearing dissimilar substituents. This differentiating impact of aggregates of compounds **1-6** on the strength of organic acids underlines the similarity with micelles of cationic surfactants [25].

However, such differentiating action of the pseudophase may be also of "trivial" nature [25]. In other words, it may be caused not by the influence of the microenvironment, but by the incomplete binding of the equilibrium species of the indicators to the aggregates.

The completeness of binding of the dye species may be estimated either by using the dependences of pK_a^{app} (or ΔpK_a^{app}) on the concentration of calixarenes (dendrimers) or by the character of alteration of absorption (emission) spectra under the same conditions. As a rule, the curves of pK_a^{app} vs. C_{calix} or C_{dendr} reach the plateau [26–28, 31], as it is exemplified in Figure 6. For instance, in solutions of **1** the concentration C_{calix} = 2.5$10^{-3}$ M is enough for obtaining stable pK_a^{app} values for the majority of dyes. Only for several more hydrophilic indicators,

constant values are fixed at higher calixarene concentrations (Table 2), etc.

Similar conclusions were deduced from the electronic spectra [26–29, 31]. The hypso- or bathochromic shifts of the absorption bands of the equilibrium species are of the same sign as on going from water to surfactant solutions (at C > CMC) or to organic solvents.

Hence, the medium effects in **1-6** solutions should be attributed to the influence of the microenvironment within the pseudophase of the positively charged aggregates.

5. Possible mechanisms of dye + calixarene association

Though the inclusion of smaller species into six-member calixarenes is well documented (as example, the system calix[6]arene hexasulfonate + 4-nitrophenol can be proposed [13]), the cage of calixarene **2** is unable to admit the whole bromophenol blue ion. Even more so, it refers to the case of calixarene **1** [26, 31]. Some possible interaction schemes are given in Figure 11. Such kinds of associates can represent the state of the dye species fixed at the colloidal aggregates of calixarene **2**.

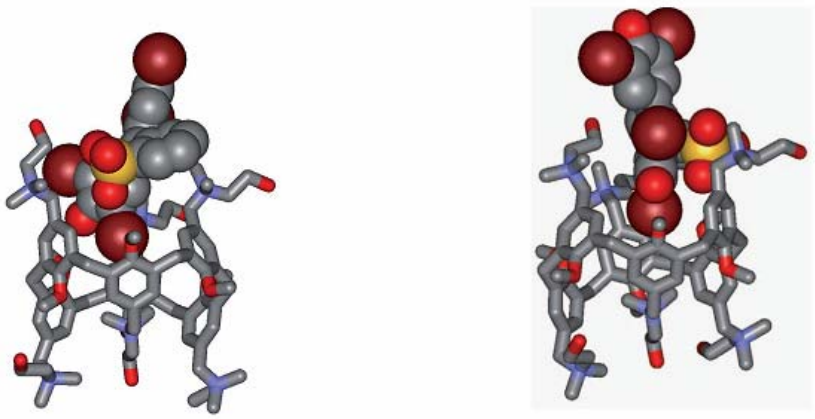

Figure 11. The possible complexes of bromophenol blue dianion, R^{2-}, with the cavity of calix[6]arene 2 (the structures are obtained using the program HyperChem 8.0 Evaluation and WebLabViewer 3.5). Reprinted from ref. 31 with permission of the American Chemical Society.

In the case of the prolonged molecule (or ion) of methyl orange, the complete docking into the cage of **2** is quite possible [31]. However, this is an exception within the set of dyes used in our studies. More probable is a partial penetration

of the dye species into the calixarene cavity or even formation of exo complexes. In Figure 12, two from a number of possible positions of 4-nitrophenol in its R^- form, fixed by a small aggregate of a four-member calixarene **1**, are schematically presented. Analogous endo and exo complexes have been constructed earlier for the R^{2-} anion of bromophenol blue [31].

Attempts to directly detect the interaction between cationic calixarene **1** and bromophenol blue were made by ^{1}H NMR spectroscopy by using a concentration range sufficiently higher than that for UV-vis spectroscopy. Unfortunately, these studies were hindered by the undesirable effect of precipitation [31].

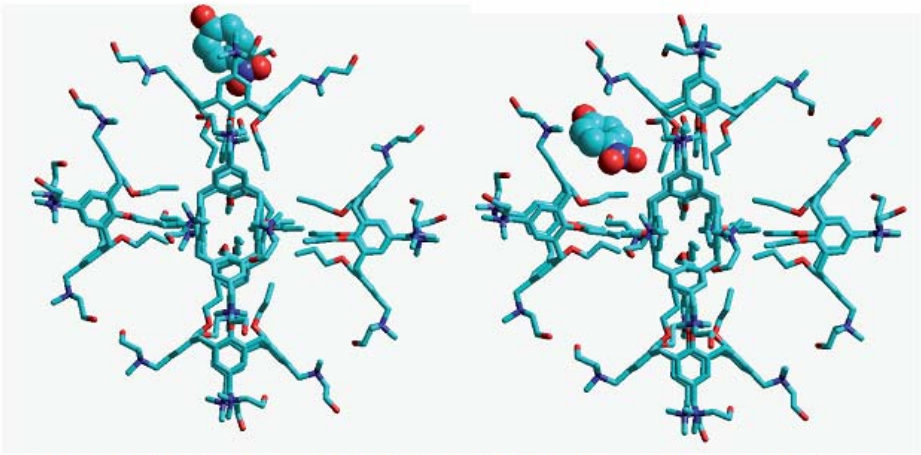

Figure 12. Endo (a) and exo (d) complexes of calixarene **1** *aggregates with the anion of 4-nitrophenol. (the structures are obtained using the program HyperChem 7.5 Evaluation) Reprinted from ref. 31.*

In the case of dendrimers, the dye species may be located in the voids of the branchy structures. Interestingly, compound **5** exerts a less expressed influence on the acid-base equilibrium of the dyes, as compared with those of **3** and **4** (Figure 6). The main reason may be the absence of *n*-dodecyl chains in its molecule.

6. The peculiarities of some physico-chemical processes in solutions containing aggregates of compounds 1-6

Within the course of our studies [26–31], we have found a number of chemical processes that demonstrate either the similarity of distinction between the calixarene and dendrimer aggregates, on the one hand, and common sphere-shaped micelles of cationic surfactants, on the other hand. Some of them are

briefly considered below.

The peculiar of methyl orange behavior. It is well known, that in the presence of small amounts of cationic surfactants, far below the CMC value, the absorption band of the anionic species of methyl orange (Figure 3) in water (λ_{max} = 462–463 nm) undergoes a dramatic hypsochromic shift up to 360–370 nm [35, 36]. This effect was explained in terms of mixed dye–surfactant micelles, where the azo dye exists in form of dimers with parallel orientation of chromophores [36]. At elevated surfactant concentrations, the band shifts toward 420–430 nm, indicating the existence of single R^- ions of the dye fixed in the micellar pseudophase (sole dye ion per micelle).

The displacement of the band to the UV-region is typical for the diluted (7.5×10^{-5} to 2.5×10^{-4} M) aqueous solutions of calixarene **1** [28], and from this viewpoint the calixarene **1** behaves in aqueous solutions like a cationic surfactant. Contrary to it, such a "dimeric" band in the UV portion of the spectrum was not registered in the case of calixarene **2** within the whole concentration range examined, from 1×10^{-5} to 0.01 M [31]. This is in line with the existence of aggregated calixarene species even at the extremely low concentrations of **2**, deduced from the DLS data. Another explanation of the absence of this indicative UV band in diluted solutions of may be the aforementioned complete penetration of the prolonged dye ion into the six-member cage of calixarene **2**. In principle, such docking can preserve the dye–dye interaction.

Interaction of dendrimers with fluorescein. Fluorescein dianion R^{2-} (Figure 5) can be protonated to form monoanion, neutral molecule, and cation. The state of the three-step ionization equilibrium in water $H_3R^+ \rightleftharpoons H_2R \rightleftharpoons HR^- \rightleftharpoons R^{2-}$ is shifted on introducing dendrimers **3** and **4** in the same direction as in micellar solutions of cationic surfactants, and the R^{2-} absorption band is also red-shifted by ca. 10 nm as compared to aqueous media [27].

The neutral species, H_2R, is known to be an equilibrium mixture of three tautomers: zwitter-ion, quinonoid, and colorless lactone (Figure 13).

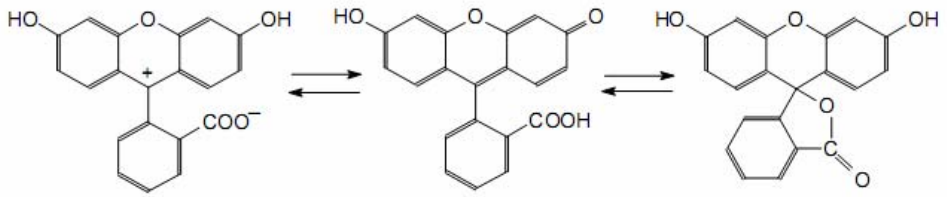

Figure 13. Zwitter-ionic, quinonoidal, and lactonic tautomers of fluorescein.

In micellar media, a drop of molar absorptivity is usually registered because

of shift of tautomeric equilibria: the zwitter-ion and quinoid tautomers convert into the colorless lactone. This effect was also registered in dendrimer solutions [27]. Surprisingly, dendrimer **4**, having a smaller number of hydrocarbon tails and possessing a higher CAC value as compared with dendrimer **3**, displays a more "micellar-like" influence on tautomeric equilibrium of fluorescein. This may be caused by a higher aggregation numbers of the less hydrophobic dendrimer **4**.

Investigation of aggregates using solvatochromic pyridinium-N-phenolate dyes. We also examined the behavior of two solvatochromic pyridinium-*N*-phenolate dyes, the so-called Reichardt's dyes (Figure 14), which can also serve as useful acid-base indicators in organized solutions.

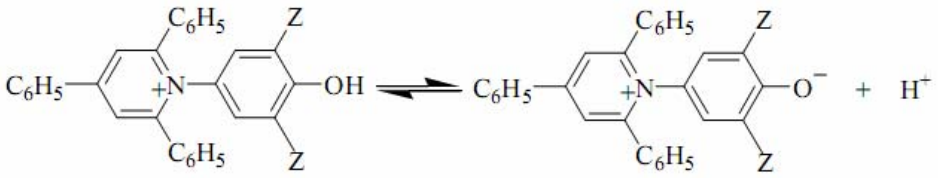

HR^+, colorless $R^{\pm}$, colored

Figure 14. Cationic and zwitter-ionic forms of pyridinium-N-phenolate dyes (Z = C_6H_5; Cl; pK_a^w = 8.64 and 4.78 respectively).

The standard dye (Z = C_6H_5) in its colored form, $R^{\pm}$, possesses = 453 nm in water [37], while in micelles of cationic surfactants is ca. 530–540 nm [37]. Analogous shift has been reported by Pan and Ford for the dendrimer of high generation, which forms in fact "unimolecular" micelles in water [38]. However, neither in solutions of low generation dendrimers **3-6** nor in the presence of aggregates of calixarenes **1** and **2** such effects were observed. For the chloro derivative in solutions of compound **3**, the value is 408 nm (in water: 412 nm) [27]. The pK_a^{app} value appeared to be even somewhat higher than in water ($\Delta pK_a^{app} = +0.3$), while in cationic micelles $\Delta pK_a^{app} = -1.0$, and the value is 465 nm [27]. Probably, the cationic species HR^+ are practically not bound by the dendrimer.

Thus, these solvatochromic dyes testify rather against the similarity between the aggregates of **1-6** and common cationic surfactant micelles.

Kinetic experiments. A preliminary decision may be made that the kinetic data also allow distinguishing between the aggregates of **1-6** and the micelles of cationic colloidal surfactants. For instance, the influence of dendrimer **3** on

the rate of the hydrolysis reaction of diacetylfluorescein shows that the local HO^- concentration in dendrimer is much lower than in the Stern layer of cationic micelles, where the rate of the same reaction is much higher:

Diacetylfluorescein (colorless) + 2 HO^- $\longrightarrow$ Fluorescein (R^{2-}, green fluorescence) (2)

On the other hand, cetyltrimethylammonium bromide micelles protect the fading of the bromophenol blue R^{2-} anion at pH around 12 (Figure 15)

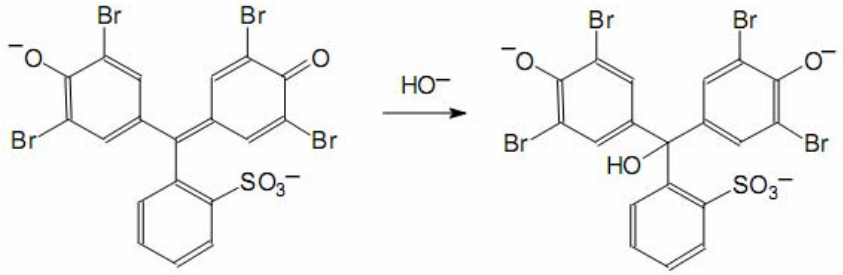

Figure 15. The conversion of the blue dianion R^{2-} to the colorless trianion ROH^{3-} as a result of the nucleophilic attack of the HO^- ion.

However, the dye fades in solutions of dendrimer **3** and of calixarene **1** and **2** just as in water.

7. Concluding remarks

In aqueous solution, cationic calixarenes and low generation dendrimers readily form positively charged aggregates. The size varies from 3–4 nm to $\approx 10^3$ nm, depending on the molecular structure. Large aggregates of calixarene **2** consist of primary ones, being at least one order of magnitude smaller. The positive charge of the particles is confirmed both by the electrokinetic measurements (e.g., for calixarenes ζ varies from +41 to +80 mV) and their influence on the pK_a values of a set of indicator dyes.

The aggregates markedly influence the absorption spectra and tautomerism of the dyes. The effects displayed by both calixarene and dendrimer aggregates resemble in outline those typical for micellar solutions of cationic surfactants. However, the agreement is far from being complete. For example, some kinetic data allow distinguishing between the aggregates under study and the common micelles of colloidal surfactants. Similar likeness with some specific differences was also stated between cationic surfactant modified silica nanoparticles [39]

and spherical polymeric polyelectrolyte brushes on the one hand and micelles of cationic amphiphiles on the other hand [40].

Concluding, on using ionic calixarenes and dendrimers in aqueous media, not the inclusion phenomena solely, but also micellar effects of colloidal aggregates should be taken into account.

Acknowledgments

We are grateful to Professor Warren T. Ford and A. A. Dissanayake, Oklahoma State University, USA, and Dr. E. Yu. Bryleva, Scientific-Technological Complex "Institute for Single Crystals", Kharkov, Ukraine for the mutual study of dendrimers [27]. We thank Dr. L. V. Kutuzova, Fakultät Angewandte Chemie, Hochschule Reutlingen, Germany and our Ukrainian colleagues Dr. Science (Chemistry) V. I. Boyko, Drs. A. B. Drapaylo, S. I. Miroshnichenko, A. P. Kryshtal, A. G. Yakubovskaya, Ph.D. student T. A. Cheipesh and former student O. Yu. Soboleva, who participated in the different stages of the above research.

References

1. *Encyclopedia of Supramolecular Chemistry*. J. L. Atwood, J. W. Steed (Eds.) Taylor & Francis, 2004.
2. Sgarlata, C.; Bonaccorso, C.; Gulino, F. G., Zito, V.; Arena, G.; Sciotto, D. *New J. Chem.* **2009**, *39*, 991–997.
3. Rodik, R. V.; Boyko, V.I.; Kalchenko, V.I. *Current Medicinal Chemistry* **2009**, *16*, 1630–1655.
4. Morozova, J. E.; Kazakova, E. Kh.; Mironova, D. A.; Shalaeva, Y. V.; Syakaev, V. V.; Makarova, N. A.; Konovalov, A. I. *J. Phys. Chem. B*, **2010**, *114*, 13152–13158.
5. Suwinska, K.; Lesnievska, B.; Wszelaka-Rylik, M.; Straver, L.; Jebors, S.; Coleman, A.W. *Chem. Comm.* **2011**, *41*, 8766–8768.
6. Rodik, R. V.; Klymchenko, A. S.; Jain, N.; Miroshnichenko, S. I.; Richert, L.; Kalchenko, V. I.; Mély, Y. *Chemistry – A Eur. J.* **2011**, *17*, 5526–5538.
7. Zhang, Y.; Pham, T. H.; Sánchez Pena, M.; Agbaria, R. A.; Warner, I. M. *Applied Spectrosc.* **1998**, *52*, 952–957.
8. Shi, Y.; Schneider, H.-J. *J. Chem. Soc., Perkin Trans. 2*, **1999**, 1797–1803.
9. Liu, Y.; Chen, Y.; Li, L.; Huang, G.; You, C.-C.; Zhang, H.-Y.; Wada, T.; Inoue, Y. *J. Org. Chem.* **2001**, *66*, 7209–7215.
10. Zhang, Y.; Cao, W. *New J. Chem.* **2001**, *25*, 483–486.

11. Liu, Y.; Han, B.-H.; Chen, Y.-T. *J. Org. Chem.* **2000**, *65*, 6227–6230.
12. Liu, Y.; Han, B.-H.; Chen, Y.-T. *J. Phys. Chem. B*, **2002**, *106*, 4678–4687.
13. Kunsági-Máte, S.; Szabo, K.; Lemli, B.; Bitter, I.; Nagy, G.; Kollár, L. *Thermochim. Acta* **2005**, *425*, 121–126.
14. Da Silva, E.; Lazar, A. N.; Coleman, A. W. *J. Drug. Sci. Tech.* **2004**, *14*, 3–20.
15. Rehm, M.; Frank, M.; Schatz, J. *Tetrahedron Lett.* **2009**, *50*, 93–96.
16. Shinkai, S.; Mori, S.; Koreishi, H.; Tsubaki, T.; Manabe, O. *J. Am. Chem. Soc.* **1986**, *108*, 2409–2416.
17. Arimori, S.; Nagasaki, T.; Shinkai, S. *J. Chem. Soc., Perkin Trans. 1*, **1993**, 887–889.
18. Lee, M.; Lee, S. J.; Jiang, L. H. *J. Am. Chem. Soc.* **2004**, *126*, 12724–12725.
19. Amirov, R.; Nugaeva, Z. T.; Mustafina, A. R.; Fedorenko, S. V.; Morozov, V. I.; Kazakova, E. Kh.; Habicher, W. D.; Konovalov, A. I. *Colloids Surf. A.* **2004**, *240*, 35–43.
20. Ukhatskaya, E. V.; Kurkov, S. V.; Matthews, S.E.; El Fagui, A.; Amiel, C.; Dalmas, F.; Loftsson, T. *Intern. J. Pharm.* **2010**, *402*, 10–19.
21. Nakai, T.; Kanamori, T.; Sando, S.; Aoyama, Y. *J. Am. Chem. Soc.* **2003**, *125*, 8465–8475.
22. Kellermann, M.; Bauer, W.; Hirsch, A.; Schade, B.; Ludwig, K.; Böttcher, C. *Angew. Chem. Int. Ed.* **2004**, *43*, 2959–2962.
23. Becherer, M.; Schade, B.; Böttcher, C.; Hirsch, A. *Chem. Eur. J.* **2009**, *15*, 1637–1648.
24. Jäger, C.M.; Hirsch, A.; Schade, B.; Ludwig, K.; Böttcher, C.; Clark, T. *Langmuir* **2010**, *26*, 10460–10466.
25. Mchedlov-Petrossyan, N. O. *Pure Appl. Chem.* **2008**, *80*, 1459–1510.
26. Mchedlov-Petrossyan, N. O.; Vilkova, L. N.; Vodolazkaya, N. A.; Yakubovskaya, A. G.; Rodik, R. V.; Boyko, V. I.; Kalchenko, V. I. *Sensors* **2006**, *6*, 962–977.
27. Mchedlov-Petrossyan, N. O.; Bryleva, E. Yu.; Vodolazkaya, N. A.; Dissanayake, A. A.; Ford, W. T. *Langmuir* **2008**, *24*, 5689–5699.
28. Mchedlov-Petrossyan, N. O.; Vodolazkaya, N. A.; Vilkova, L. N.; Soboleva, O. Yu.; Kutuzova, L. V. ; Rodik, R. V.; Miroshnichenko, S. I.; Drapaylo, A. B. *J. Mol. Liquids* **2009**, *145*, 197–203.
29. Mchedlov-Petrossyan, N. O.; Bogdanova, L. N.; Rodik, R. V.; Vodolazkaya, N. A.; Kutuzova, L. V.; Kalchenko, V. I. *Rep. Nat. Acad. Sci. Ukraine* **2010**, No. 3, 148–153.

30. Mchedlov-Petrossyan, N. O. *Voprosy Khimiyi i Khimicheskoi Tekhnologiyi (The Questions of Chemistry and Chemical Technology)* **2011**, No. 4 (2), 82–84.
31. Mchedlov-Petrossyan, N. O.; Vodolazkaya, N. A.; Rodik, R. V.; Bogdanova, L. N.; Cheipesh, T. A.; Soboleva, O. Yu.; Kryshtal, A. P.; Kutuzova, L. V.; Kalchenko, V. I. *J. Phys. Chem. C* **2012**, *116*, 10245–10259.
32. Arimori, S.; Nagasaki, T.; Shinkai, S. *J. Chem. Soc., Perkin Trans. 2*, **1995**, 679–683.
33. Shahgaldian, P.; Sciotti, M. A.; Pieles, U. *Langmuir,* **2008**, *24*, 8522–8526.
34. Arimura, T.; Kawabata, H.; Matsuda, T.; Muramatsu T.; Satoh H.; Fujio K.; Manabe, O.; Shinkai, S. *J. Org. Chem.,* **1991**, *56*, 301–306.
35. Quadrifoglio, F.; Crescenzi, V. *J. Colloid Interface Sci.* **1971**, *35*, 447–459.
36. Reeves, R. L.; Harkaway, S. A. in: *Micellization, solubilization, and microemulsions*, K. L. Mittal (Ed.), Russian transl. Mir, Moscow, 1980.
37. Reichardt, C.; Welton, T. *Solvents and Solvent Effects in Organic Chemistry;* Wiley–VCH: Weinheim, 2011.
38. Pan, Y.; Ford, W. T. *Macromolecules* **2000**, *33*, 3731–3738.
39. Bryleva, E. Yu.; Vodolazkaya, N. A.; Mchedlov-Petrossyan, N. O.; Samokhina, L. V.; Matveevskaya, N. A.; Tolmachev, A. V. *J. Colloid Interface Sci.* **2007**, *316*, 712–722.
40. Vodolazkaya, N. A.; Mchedlov-Petrossyan, N. O.; Bryleva, E. Yu.; Biletskaya, S. V.; Schrinner, M.; Kutuzova, L. V.; Ballauff, M. *Functional Materials* **2010**, *17*, 470–476.